JOURNAL OF COMPUTATIONAL PHYSICS 108, 38–50 (1993)

An Adaptive Grid with Directional Control

J. U. BRACKBILL

Los Alamos National Laboratory, Los Alamos, New Mexico 87545

Received August 27, 1992

A variational formulation of Winslow's variable diffusion method is combined with a directional control functional to derive an adaptive grid generator for adaptive node movement. The addition of directional control allows one to align mesh lines with a prescribed vector field while adapting the spacing to resolve the data. It is shown that harmonic function theory can be applied to define the conditions under which unique solutions of the resulting elliptic equations exist. The grid generator is applied to the complex problem of magnetic field reconnection driven by fluid instability. The results demonstrate that the cost of a computation with an adaptive grid with directional control is only one-tenth of the cost of either a calculation on an Eulerian grid or on an adaptive grid without directional control.

INTRODUCTION

Experience has shown that an adaptive computation mesh increases the accuracy and decreases the cost of numerical calculations. When the mesh adapts to resolve local gradients, a smaller number of zones is required than with a uniform mesh. Adaptivity is achieved in various ways, for example by using moving finite elements [1] mesh refinement [2–5], or by adaptive node movement [6–8]. A new method for adaptive node movement is presented here. With node movement, a fixed number of nodes with fixed connectivity is moved within the computational domain to increase numerical accuracy. In a recent review of adaptive meshes of this type, it is noted that "these methods are applicable to the solution of non-stationary flow problems that contain moving regions of rapid change in the flow variables, surrounded by regions of relatively smooth variation" [9].

On almost every aspect of adaptive meshes, there is a variety of opinions. There are many formulations of adaptive meshes and of the objective functions that are used to drive them. There is, however, agreement that an adaptive mesh should be continuous and differentiable with nonvanishing Jacobian [10]. One reliable way to generate such a mesh is by solving elliptic equations to generate body-fitted coordinates [11], which "transform the irregular physical mesh to a square computational domain" [2]. One objection to adaptive meshes, however, is very serious if true. Altas and Stephenson comment that "a major deficiency of some of the adaptive algorithms using this approach... is a lack of control of mesh skewness in the physical domain." [2]

One can generate an orthogonal mesh and eliminate mesh skewness by solving Laplace's equation to transform the computational domain to the physical domain [12]. However, it is not clear that an orthogonal mesh also can be an adaptive mesh. Ryskin and Leal point out that there are *three independent elements of the metric tensor in two* dimensions, one of these is constrained by an integrability condition and the other two must be constrained to give orthogonality [12]. No additional degrees of freedom are available for adaptive node movement. (This is consistent with results using a variational formulation which combined adaptivity with orthogonality [6]. Experiments indicate that increased orthogonality is achieved at the expense of adaptivity.)

It is argued that orthogonality is necessary because a skewed mesh causes truncation error in numerical differentiation. However, an analysis of the effect of skewness on the accuracy of one difference equation indicates that the truncation error arising from skewness is less than that from nonuniform spacing as long as the departure from orthogonality is less than 45° [11]. A more complex analysis of truncation error in modeling convection in curvilinear coordinates supports this view [13]. While it is true that grid skewness contributes to truncation error, variation in mesh spacing and misalignment of the grid with the direction of flow also contribute. Among the properties which affect accuracy are "grid size, grid size ratio, angle between the grid lines, angle of velocity vector relative to the grid line, grid uniformity and skewness, and derivatives of the flow properties" [13], in other words, more properties than there are independent elements of the metric tensor for the mesh [14]. Clearly, no single property of the grid can be singled out in this analysis as the most important, except,

0021-9991/93 $5.00

perhaps, that the mesh be as smooth as possible, i.e., that the variation in the metric from point to point be bounded. The complexity of the problem only increases if one includes the many ways to derive difference equations for curvilinear coordinates [11, 15, 16].

Because so many different properties of the mesh seem to be important, we continue to explore elliptic generators derived from a variational formulation in which functionals describing various properties of the mesh are combined to give the desired result. This is a similar approach to that in Brackbill and Saltzman (BS), where a variational method is described which combines functionals measuring the smoothness, volume distribution, and orthogonality of the mesh [6]. The relative contributions of each of these functionals is determined by a user prescribed weight. In the present work, we use different functionals to control the properties of the mesh from those used in the BS algorithm.

Our new formulation addresses various difficulties encountered in using the BS method. In the BS method, it is difficult to characterize the ellipticity of the equations for all values of the parameters and this is reflected in the failure of the generator to give acceptable results under certain conditions [6]. Further, the terms are not dimensionally homogeneous and must be rescaled for each application [17]. This can be a serious difficulty, because of the need for tinkering to determine the correct scaling.

In our further exploration of the variational method, we seek to reduce the need for tinkering and to increase the robustness of the mesh generator while retaining the control of mesh properties offered by the BS method. The goal is to make adaptive mesh generation automatic and reliable. We have been guided by a recent paper by Dvinsky [18], which suggests the possibility that harmonic function theory may provide a general framework for developing useful mesh generators. Our new approach is to replace the smoothness and weighted volume functions, whose role in the BS method is to regularize the equations and enable adaptivity, by a functional suggested by Winslow [19] and a functional measuring the alignment of the mesh with a specified vector field [20]. It is shown that the grid generated by minimizing weighted smoothness is homeomorphic with a regular rectilinear grid. The weighted smoothness is combined with a functional measuring the alignment of the grid with a specified vector field to derive generator equations that yield both adaptivity and directional control. The functionals easily can be made dimensionally homogeneous, and the range of a single dimensionless parameter controlling the relative contribution of the two functionals can be defined precisely.

In outline, we first discuss harmonic function theory and its application to mesh generation. We then turn to Winslow's "variable diffusion" method and examine both the existence and the properties of solutions. We explore the method of aligning the mesh, show how it fits into the general framework of harmonic function theory, and present a mesh generator that combines adaptivity and directional control. We conclude with a computational example in two dimensions, illustrating the dramatic increase in computational efficiency that results from combining adaptivity and directional control.

1. APPLICATION OF HARMONIC FUNCTION THEORY TO GRID GENERATION

a. *A Review of Harmonic Function Theory*

Recently, Dvinsky has applied the theory of harmonic maps to a standard problem in grid generation, namely the generation of a mapping from a region in D in physical space (x^1, x^2, x^3) with boundary ∂D to a region R in natural space (ξ^1, ξ^2, ξ^3), with boundary ∂R [18]. The theory of harmonic maps can be used to establish the existence and uniqueness of solutions to the generator equations.

Let d^{kj} denote a specified contravariant metric in the coordinates x, $ds^2 = d^{kj}\,dx_k\,dx_j$, $d = \det\{d_{ij}\}$, and $r_{\alpha\beta}$ a specified covariant metric in the coordinates ξ, $ds^2 = r_{\alpha\beta}\,d\xi^\alpha\,d\xi^\beta$. Following Dvinsky, we define the energy density for a mapping $x: D \to R$,

$$e(\xi) = \frac{1}{2}\,d^{ij}(x)\,r_{\alpha\beta}\frac{\partial\xi^\alpha}{\partial x^i}\frac{\partial\xi^\beta}{\partial x^j}, \tag{1.1}$$

where repeated indices are summed over unless otherwise noted. Similarly to Dvinsky, we propose to specify the metrics d^{ij} and $r_{\alpha\beta}$, and then solve for the transform that maps D onto R with the specified metrics by minimizing the total energy,

$$E(\xi) = \frac{1}{2}\int_D d^3x\,\sqrt{d}\,d^{ij}r_{\alpha\beta}\frac{\partial\xi^\alpha}{\partial x^i}\frac{\partial\xi^\beta}{\partial x^j}. \tag{1.2}$$

In specifying the metrics, we require that d^{ij} and $r_{\alpha\beta}$ be symmetric, and that $\det\{d_{ij}\} > 0$.

Dvinsky applies the Hamilton–Schoen–Yau (HSY) theorem to this problem, which states:

HSY THEOREM. *Let D with metric d_{ij} and R with metric r_{ij} be two Riemannian manifolds with boundaries ∂D and ∂R and let $\phi: D \to R$ be a diffeomorphism. For any map, $f: D \to R$ such that $f|_{\partial D} = \phi|_{\partial D}$, we define $E(f) = \int_D \|df\|^2\,d^3x$. The mapping f is harmonic if it is an extremal of E.*

The Euler–Lagrange equations, whose solution minimizes the energy, Eq. (1.2), are given by

$$\frac{1}{\sqrt{d}}\frac{\partial}{\partial x^i}\sqrt{d}\,d^{ij}\frac{\partial\xi^\lambda}{\partial x^j} + d^{ij}\begin{Bmatrix}\lambda\\ \alpha\beta\end{Bmatrix}\frac{\partial\xi^\alpha}{\partial x^i}\frac{\partial\xi^\beta}{\partial x^j} = 0, \tag{1.3}$$

where $\left\{{\lambda \atop \alpha\beta}\right\}$ is the Christoffel symbol of the second kind,

$$\begin{Bmatrix}\lambda\\ \alpha\beta\end{Bmatrix} = \frac{1}{2}r^{\lambda\rho}\left[\frac{\partial r_{\rho\alpha}}{\partial x^\beta} + \frac{\partial r_{\rho\beta}}{\partial x^\alpha} - \frac{\partial r_{\alpha\beta}}{\partial x^\rho}\right]. \tag{1.4}$$

A second theorem guarantees the uniqueness of this mapping:

THEOREM. *If the curvature of R is non-positive, and ∂R is convex (with respect to the metric $r_{\alpha\beta}$) then there exists a unique harmonic map $f: x \to r$ such that f is an homotopy equivalent to ϕ. In other words, one can deform f to ϕ by constructing a continuous family of maps $g_t: D \to R$, $t \in [0, 1]$, such that $g_0(x) = \phi(x)$ and $g_t(x) = f(x)$, $\forall x \in \partial D$, $t \in [0, 1]$.*

Harmonic function theory is described by one author as generalizing harmonic functions to include mappings from curvilinear coordinates to curvilinear coordinates [21]. However, many formulations of grid generator equations restrict R, the computational domain, to Euclidean geometry,

$$R = \{(\xi^1, \xi^2, \xi^3) \mid 1 < \xi^1 < I, 1 < \xi^2 < J, 1 < \xi^3 < K\}. \quad (1.5)$$

When R is Euclidean, its curvature is zero and the second theorem guarantees the suitability of the mapping. This corresponds to the case considered by Mastin and Thompson [10], with $r_{\alpha\beta} = \delta_{\alpha\beta}$, and the total energy given by

$$E(\xi) = \int_D d^3x \sqrt{d}\, d^{ij} \frac{\partial \xi^\alpha}{\partial x^i} \frac{\partial \xi^\beta}{\partial x^j}. \quad (1.6)$$

With a Euclidean metric, $\left\{ {\lambda \atop \alpha\beta} \right\} = 0$, the Euler equations become

$$\frac{1}{\sqrt{d}} \frac{\partial}{\partial x^i} \sqrt{d}\, d^{ij} \frac{\partial \xi^\lambda}{\partial x^j} = 0. \quad (1.7)$$

b. *Natural Boundary Conditions*

Usually one solves Eq. (1.7) with Dirichlet boundary conditions. However, the natural boundary conditions for Eq. (1.7), those for which the boundary contribution to the variation is zero, are not Dirichlet. The natural boundary conditions are derived in the usual way by writing the first variation of $E(\xi)$ and integrating by parts. The boundary contribution to the variation in energy is thus found to be

$$\delta E(\xi)_{bdy} = \int_D d^3x \frac{\partial}{\partial x^i} \left[d^{ij} \frac{\partial \xi^\alpha}{\partial x^j} \delta \xi^\alpha \right]. \quad (1.8)$$

Where the metric between computational and physical coordinates is defined by

$$g^{ij} = \frac{\partial \xi^i}{\partial x^\alpha} \frac{\partial \xi^j}{\partial x^\alpha}, \quad (1.9)$$

one can write this term in the form

$$\delta E(\xi)_{bdy} = \int d^3\xi \frac{\partial}{\partial \xi^\gamma} \left[\sqrt{g}\, d^{ij} \frac{\partial \xi^\gamma}{\partial x^i} \frac{\partial \xi^\alpha}{\partial x^j} \delta \xi^\alpha \right]. \quad (1.10)$$

As prescribed by Eq. (1.5), the domain is bounded by surfaces of constant ξ^1, ξ^2, or ξ^3. For example, on a surface of constant ξ^γ the natural boundary conditions require

$$d^{ij} \frac{\partial \xi^\gamma}{\partial x^i} \frac{\partial \xi^\alpha}{\partial x^j} = 0, \qquad \alpha \neq \gamma. \quad (1.11)$$

In the simplest case, d^{ij} corresponds to a Euclidean space, $d^{ij} = \delta^{ij}$, and the natural boundary conditions on surfaces of constant ξ^γ are equivalent to requiring orthogonality at the boundary,

$$\nabla \xi^\gamma \cdot \nabla \xi^\alpha = 0, \qquad \alpha \neq \gamma. \quad (1.12)$$

The orthogonality condition can be expressed in terms of the covariant derivative using the identity

$$\nabla \xi^\alpha = \frac{\{(\partial \mathbf{x}/\partial \xi^\beta) \times (\partial \mathbf{x}/\partial \xi^\gamma)\}}{\sqrt{g}} \varepsilon_{\alpha\beta\gamma}, \quad (1.13)$$

where $\varepsilon_{\alpha\beta\gamma}$ is the Levi–Civitas tensor. Substituting this identity into Eq. (1.12) one finds

$$\nabla \xi^\gamma \cdot \nabla \xi^\alpha = \nabla \xi^\gamma \cdot \frac{\{(\partial \mathbf{x}/\partial \xi^\beta) \times (\partial \mathbf{x}/\partial \xi^\gamma)\}}{\sqrt{g}} \varepsilon_{\alpha\beta\gamma}. \quad (1.14)$$

Thus, the natural boundary conditions are satisfied if $\nabla \xi^\gamma$ and $\partial \mathbf{x}/\partial \xi^\gamma$ are collinear.

c. *Discussion*

Equation (1.7) is Laplace's equation in curvilinear coordinates where ξ^λ is any scalar [22, p. 170]. Solutions to this equation are harmonic functions giving a continuous, one-to-one mapping with continuous inverse, which is differentiable and has a non-zero Jacobian [10]. Problems are routinely solved in this way to generate grids for airfoils where the boundary of the physical domain is non-convex. For example, see the cover of *Numerical Grid Generation* [11] and many other examples within. Further, there is evidence that mapping in the reverse direction will fail for non-convex physical domains [12, 18, 23].

The interest in harmonic function theory from the viewpoint of grid generation is in the idea which Dvinsky discusses [18], that one is free to specify d^{ij} as a function of the physical coordinates when defining the energy, Eq. (1.2), and that minimizing that energy will result in a harmonic mapping with the desired metric and the same robustness as

the method of body-fitted coordinates. This is different from the method of Ryskin and Leal, who proposed specifying the metric of the transformation from computational to physical coordinates to generate orthogonal meshes [12].

We remark that inhomogenous functions of the natural coordinates may be added to Laplace's equation, as is proposed by Thompson, and that the solutions will be harmonic functions, provided the functions are of the form of the second term in Eq. (1.3). Thus, by guiding the choice of the form of the mesh control functions, the theory of harmonic functions extends the grid generation theory presented by Mastin and Thompson [11].

2. ADAPTIVE GRID GENERATORS

a. *Winslow's Variable Diffusion Equation*

We now consider the mapping generated by minimizing the functional,

$$I_s = \sum_{j=1}^{3} \int d^3x \frac{1}{w} [\nabla \xi^j]^2, \tag{2.1}$$

with weight $w = w(x^1, x^2, x^3)$ prescribed or derived from the data. The weight is everywhere positive, $w > 0$. The Euler–Lagrange equations whose solution minimizes I_s are

$$\nabla \cdot \frac{1}{w} \nabla \xi^j = 0, \qquad j = 1, 2, 3. \tag{2.2}$$

These equations are the generator equations suggested by Winslow, which he called the variable diffusion method [19]. Several authors have considered these equations [24–26], and several have also given the corresponding variational form [27, 28]. There has also been extensive experience in the application of these generator equations [27, 29, 32].

b. *Existence of Solutions*

We now show that the generator suggested by Winslow is a special case of the more general problem described by Dvinsky for which the Hamilton–Schoen–Yau (HSY) theorem applies. One recognizes that the energy $E(\xi)$, Eq. (1.2), and the functional I_s, Eq. (2.1), are identical when the metric in (1.2) and w in (2.1) are related by

$$\sqrt{d}\, d^{ij} = \frac{1}{w} \delta^{ij} \tag{2.3}$$

and thus that the HSY theorem applies. Further, substituting this metric into Winslow's equations yields Eq. (1.7). Thus, by the HSY theorem, solutions ξ^λ to the Winslow equation are harmonic. That is, the Jacobian of the mapping does not vanish in D, and the mapping is one to one and onto.

c. *Solving the Generator Equations*

To solve the Euler equations numerically, one usually interchanges dependent and independent variables. As written, the solution of the Euler equations, Eq. (2.2), requires evaluating derivatives of (ξ^1, ξ^2, ξ^3) with respect to the physical coordinates (x^1, x^2, x^3). In grid generation, however, one usually specifies the logical arrangement of grid points and computes the physical coordinates of the grid points. Thus, (ξ^1, ξ^2, ξ^3) must be made the independent variables.

We interchange the dependent and independent coordinates in Eq. (2.2) as follows: First, we perform the indicated differentiation of w in Eq. (2.2),

$$\nabla^2 \xi^j = \frac{\nabla w}{w} \cdot \nabla \xi^j, \qquad j = 1, 2, 3. \tag{2.2'}$$

We use the chain rule to express the right-hand side of Eq. (2.2′) in terms of derivatives with respect to the natural coordinates,

$$\nabla w \cdot \nabla \xi^j = \frac{\partial w}{\partial \xi^i} g^{ij}, \tag{2.4}$$

where g^{ij} is defined by Eq. (1.9). Using the identity, $\nabla^2 \mathbf{x} = 0$, as in Ref. [12, p. 116], we find

$$\nabla^2 \xi^k = -\, g^{ij} \frac{\partial^2 \mathbf{x}}{\partial \xi^i \partial \xi^j} \cdot \nabla \xi^k. \tag{2.5}$$

We then substitute Eq. (2.5) into Eq. (2.2′) to obtain

$$-\, g^{ij} w \frac{\partial^2 \mathbf{x}}{\partial \xi^i \partial \xi^j} \cdot \nabla \xi^k = g^{ik} \frac{\partial w}{\partial \xi^i}. \tag{2.6}$$

One can then use the relation

$$\nabla \xi^i \cdot \frac{\partial \mathbf{x}}{\partial \xi^j} = \delta_{ij} \tag{2.7}$$

to derive the homogeneous equations,

$$g^{ij} \frac{\partial}{\partial \xi^i} w \frac{\partial \mathbf{x}}{\partial \xi^j} \cdot \nabla \xi^k = 0, \qquad k = 1, 2, 3, \tag{2.8}$$

for the natural components of the physical coordinates. Since g is not zero, this system of equations for the natural

components of the physical coordinates can be replaced by the autonomous equations

$$g^{ij}\frac{\partial}{\partial \xi^i} w \frac{\partial \mathbf{x}}{\partial \xi^j} = 0 \tag{2.9}$$

for the Cartesian components of the physical coordinates.

d. *Properties of Solutions of Winslow's Equations*

A geometric interpretation of Eq. (2.2′) suggests more generally how the adaptive grid resolves gradients in the data. The right-hand side of Eq. (2.2′) is the component of the gradient of w in a direction perpendicular to surfaces of constant ξ^1, ξ^2, and ξ^3, for $j = 1, 2, 3$, respectively. Thus, the variation in spacing between level surfaces of the natural coordinates measured by the left side of Eq. (2.2′) is proportional to the component of the gradient of w normal to the surface measured by the right side of Eq. (2.2′). When w is a constant, the solution is the one with the least variation permitted by the boundary conditions, commonly called body-fitted coordinates [29]. When w is not constant, but instead is defined by the user to control the mesh spacing, the solution is one with variation depending upon w.

The form of w depends on the specific application. For example, if one wishes to resolve gradients of a variable U, w will then be of the following form:

$$w = |\nabla U|/|U|. \tag{2.10}$$

If one wishes to have an equal number of simulation particles, n, in each cell, one can define $w = n$. We note that a constant gradient or constant n will not result in any variation of the mesh spacing.

The weight function can be used also to generate grids in curvilinear coordinates. For example, toroidal geometry requires that the solutions of the generator equations reflect the curvilinear coordinates of the torus. To do this, one may define the weight function so that the Cartesian equations generate a toroidal mesh. For example, the weight $w = rR$, where R is the major radius and r is the minor radius, gives a mesh with equal spacing in the minor radius r, the poloidal angle θ, and the toroidal angle ϕ [31]. A weight that gives both curvilinear coordinates and adaptivity is formed by multiplying the geometric and adaptive weights.

Eiseman [25] and Tu and Thompson [26] have suggested the use of vector weight functions whose contravariant components (w^1, w^2, w^3) determine the spacing between corresponding level curves of ξ^1, ξ^2, and ξ^3. One might expect this approach to eliminate clustering of grid points in a direction perpendicular to the gradient, which can occur with the Winslow formulation, while leaving the orientation of the grid lines with the gradient unchanged.

3. AN ADAPTIVE GRID WITH DIRECTIONAL CONTROL

a. *Directional Control Functional*

Giannakopoulos and Engel have demonstrated in two dimensions the ability to cause grid lines to align with a prescribed vector field [20]. Alignment can be very useful when there is a natural anisotropy in the problem, for example in problems with a dominant flow direction or in magnetized plasmas. The geometric interpretation of Eq. (2.2′) suggests that directional control and adaptivity be combined. That is, if the grid can be oriented so that adaptivity affects the spacing of only one set of level curves, the effectiveness of adaptivity in two or three dimensions can approach the effectiveness in one dimension. The functional I_d to control the alignment of the mesh with adaptive weighting is written

$$I_d = \int d^3\mathbf{x}\,\frac{1}{w}\left\{(\mathbf{A}\times\nabla\xi^1)^2 + (\mathbf{B}\times\nabla\xi^2)^2 + (\mathbf{C}\times\nabla\xi^3)^2\right\} \tag{3.1}$$

with three prescribed vector fields, **A**, **B**, and **C**. Minimizing I_d results in increased alignment of the normals to grid surfaces of constant ξ^1, ξ^2, and ξ^3 with the vectors **A**, **B**, and **C**, respectively. When **A**, **B**, and **C** are mutually orthogonal, the tangent vector, $\mathbf{x}_{\xi^1}$, will be aligned with $\mathbf{B}\times\mathbf{C}$, the tangent vector, $\mathbf{x}_{\xi^2}$, will be aligned with $\mathbf{C}\times\mathbf{A}$, and the tangent vector, $\mathbf{x}_{\xi^3}$, will be aligned with $\mathbf{A}\times\mathbf{B}$.

The functional I_d in Eq. (3.1) and the energy integral E in Eq. (1.2), are identical for a particular choice of metric. By substituting the vector identity into Eq. (3.1), where **V** is any of **A**, **B**, or **C**, we find that the metric for the term becomes

$$\sqrt{d_v}\,d_v^{ij} = \frac{1}{w}\left\{V_k V_k \delta^{ij} - V^i V^j\right\} \tag{3.3}$$

and that the corresponding energy integral is written

$$E(\xi) = \int d^3x \left[\sqrt{d_A}\,d_A^{ij}\frac{\partial\xi^1}{\partial x^i}\frac{\partial\xi^1}{\partial x^j} + \sqrt{d_B}\,d_B^{ij}\frac{\partial\xi^2}{\partial x^i}\frac{\partial\xi^2}{\partial x^j} + \sqrt{d_C}\,d_C^{ij}\frac{\partial\xi^3}{\partial x^i}\frac{\partial\xi^3}{\partial x^j}\right]. \tag{3.4}$$

The Euler equations whose solutions minimize the energy E in Eq. (3.4) are in the standard form Eq. (1.7). Thus, the HSY theorem applies to the directional control generator. In vector form, the Euler equations are written

$$-\nabla\frac{\mathbf{A}\cdot\mathbf{A}}{w}\nabla\xi^1 + \left\{\nabla\cdot\frac{1}{w}\mathbf{AA}\right\}\cdot\nabla\xi^1 = 0, \tag{3.5a}$$

$$-\nabla\frac{\mathbf{B}\cdot\mathbf{B}}{w}\nabla\xi^2 + \left\{\nabla\cdot\frac{1}{w}\mathbf{BB}\right\}\cdot\nabla\xi^2 = 0, \tag{3.5b}$$

$$-\nabla\frac{\mathbf{C}\cdot\mathbf{C}}{w}\nabla\xi^3 + \left\{\nabla\cdot\frac{1}{w}\mathbf{CC}\right\}\cdot\nabla\xi^3 = 0. \tag{3.5c}$$

From Eq. (1.11), which gives the general form of the natural boundary conditions, and Eq. (3.3), which gives the metric for directional control, the natural boundary conditions for Eqs. (3.5) on a surface of constant ξ^1, for example, are

$$(\mathbf{B}\times\nabla\xi^1)\cdot(\mathbf{B}\times\nabla\xi^2)=(\mathbf{C}\times\nabla\xi^1)\cdot(\mathbf{C}\times\nabla\xi^3)=0. \quad (3.6)$$

The boundary contribution is zero if (a) $\mathbf{B}=0$ and $\mathbf{C}=0$, or (b) $\mathbf{B}$ is parallel to $\nabla\xi^2$ and $\mathbf{C}$ is parallel to $\nabla\xi^3$. One derives similar conditions for the other boundaries.

Once again, to solve the Euler equations, one interchanges dependent and independent variables using the identity

$$(\mathbf{A}\cdot\nabla)(\mathbf{A}\cdot\nabla)\mathbf{x}=(\mathbf{A}\cdot\nabla)\mathbf{A} \quad (3.7)$$

and the chain rule to derive

$$(\mathbf{A}\cdot\nabla)(\mathbf{A}\cdot\nabla)\mathbf{x}=(\mathbf{A}\cdot\nabla\xi^i)(\mathbf{A}\cdot\nabla\xi^j)\frac{\partial^2\mathbf{x}}{\partial\xi^i\,\partial\xi^j}+(\mathbf{A}\cdot\nabla\mathbf{A})\cdot\nabla\xi^j\frac{\partial\mathbf{x}}{\partial\xi^j}+\mathbf{A}\cdot\{(\mathbf{A}\cdot\nabla)\nabla\xi^j\}\frac{\partial\mathbf{x}}{\partial\xi^j}. \quad (3.8)$$

By forming the scalar product of Eq. (3.8) with $\nabla\xi^1$ and using Eq. (2.7), one derives the identity

$$\mathbf{A}\cdot\{(\mathbf{A}\cdot\nabla)\nabla\xi^1\}=-(\mathbf{A}\cdot\nabla\xi^i)(\mathbf{A}\cdot\nabla\xi^j)\frac{\partial^2\mathbf{x}}{\partial\xi^i\,\partial\xi^j}\nabla\xi^1. \quad (3.9)$$

Substituting the identity, Eq. (3.9), into the Euler equations, Eqs. (3.5a)–(3.5c), one finds

$$\left\{G_A^{ij}\left(\frac{\partial}{\partial\xi^i}w\frac{\partial\mathbf{x}}{\partial\xi^j}\right)-w[\nabla(\mathbf{A}\cdot\mathbf{A})-\nabla\cdot\mathbf{AA}]\right\}\cdot\nabla\xi^1=0 \quad (3.10a)$$

$$\left\{G_B^{ij}\left(\frac{\partial}{\partial\xi^i}w\frac{\partial\mathbf{x}}{\partial\xi^j}\right)-w[\nabla(\mathbf{B}\cdot\mathbf{B})-\nabla\cdot\mathbf{BB}]\right\}\cdot\nabla\xi^2=0 \quad (3.10b)$$

$$\left\{G_C^{ij}\left(\frac{\partial}{\partial\xi^i}w\frac{\partial\mathbf{x}}{\partial\xi^j}\right)-w[\nabla(\mathbf{C}\cdot\mathbf{C})-\nabla\cdot\mathbf{CC}]\right\}\cdot\nabla\xi^3=0, \quad (3.10c)$$

where G_A^{ij}, for example, is defined by

$$G_A^{ij}=\mathbf{A}\cdot\mathbf{A}g^{ij}-(\mathbf{A}\cdot\nabla\xi^i)(\mathbf{A}\cdot\nabla\xi^j). \quad (3.11)$$

These equations give the contravariant components of the physical coordinates and require the solution of a coupled system to calculate the position of the grid points. A linear system of equations must then be solved for the physical components. Note that the equations are unchanged when $-\mathbf{A}$ is substituted for $\mathbf{A}$, $-\mathbf{B}$ for $\mathbf{B}$, or $-\mathbf{C}$ for $\mathbf{C}$.

b. *Regularization*

A geometric interpretation of the alignment functional uncovers a difficulty. The functional in Eq. (3.1) is minimized when the variation in ξ^1 is in the direction $\mathbf{A}$, no matter what that variation in ξ^1 may be. Thus, when the grid is oriented in a direction $\mathbf{A}$ the variation in ξ^1 is undetermined.

The difficulty can be identified within the theory of harmonic functions reviewed in Section 1. For example, when $\nabla\xi^1$ is aligned with $\mathbf{A}$, the determinant $d_A=0$, the energy in Eq. (3.4) has no extremum with respect to variations in ξ^1, and Eq. (3.10a) has no solution.

This difficulty can be avoided by regularizing the equations as follows. Since Eqs. (2.8) and (3.10) are derived by minimizing functionals of similar form, the "Winslow" and "orientation" functionals can be combined. The two functions have the same dimensionality if each reference vector is made non-dimensional. In the examples below we divide each reference vector by its maximum magnitude. This has the advantage that the difficulty in scaling the contributions of the two independent functionals is eliminated. A functional combining adaptivity and directional control then can be written

$$I=(1-\Gamma)I_s+\Gamma I_d, \quad (3.12)$$

where $0\leqslant\Gamma<1$ is a user-specified, non-dimensional constant to control the degree of alignment of the grid with the reference vectors. Increasing Γ increases the alignment of the grid with the reference vectors.

4. DRIVEN MAGNETIC RECONNECTION IN TWO DIMENSIONS

To illustrate the properties of the adaptive grid with directional control, we model an unstable plasma flow in two dimensions with the particle-in-cell magnetohydrodynamic code, FLIP-MHD [32]. Flow of a plasma in a magnetic field is an example of a naturally occurring problem with significant anisotropy, in which the magnetic field introduces a preferred direction. The example illustrates the dramatic increase in computational efficiency when one uses an adaptive grid with directional control.

We examine an unstable shear flow, and its effect on magnetic field topology. We model the evolution of the instability from an initial state on a two-dimensional domain with rigid free-slip boundaries at $x=0$ and $x=L$ and periodic boundary conditions in y with periodic

length L. Initially, the velocity and magnetic field depend only on x,

$$\frac{u_y}{u_0}, \frac{b_y}{b_0} = 2 \tanh\left[\frac{(x - L/2)}{\delta}\right] - 1, \tag{4.1}$$

with $\delta = L/30$. The flow is subsonic and super-Alfvenic,

$$\frac{u_0}{\sqrt{p/\rho}} = 0.5, \qquad \frac{u_0}{\sqrt{b^2/\sqrt{\rho}}} = 10. \tag{4.2}$$

where $\mathbf{b}$ is the magnetic field intensity and ρ is the mass density. The shear viscosity, μ, corresponds to a Reynolds number, Re = 4000, and the resistivity, η, corresponds to a magnetic Reynolds number, Rm = 1000, where Re and Rm are defined using the full channel width,

$$\mathrm{Re} = \frac{u_0 L}{\mu}, \qquad \mathrm{Rm} = \frac{u_0 L}{\eta}. \tag{4.3}$$

For this problem, the estimated dissipation length scale, d, at steady state is $d = 0.011L$ [33]. To resolve this scale length, the grid spacing must be $O(d)$, which requires for this problem a uniform grid with 90×90 zones. We observe that a sequence of numerical calculations with increasing resolution converges as the mesh spacing approaches this value, and in our comparison of various mesh strategies, the comparison is of the rate of convergence and of the effort required to achieve convergence.

The growth of the Kelvin–Helmholtz instability results in the formation of eddies in the flow, which are illustrated in Fig. 1, a plot of streamlines at $t = 2.2L/u_0$ from a calculation with 120 zones in x and 120 in y (120×120). It has been shown that an eddy expels a magnetic field from the interior of an eddy and causes it to intensify at the periphery [34]. A well-developed example of this phenomenon is shown in Fig. 2, where the magnetic field lines (contours of constant $\mathbf{a}$, $\mathbf{b} = \nabla \times \mathbf{a}$) define three regions bounded by closed field lines. Two of these were present in the original problem and lie on either side of the boundary layer. The third has been

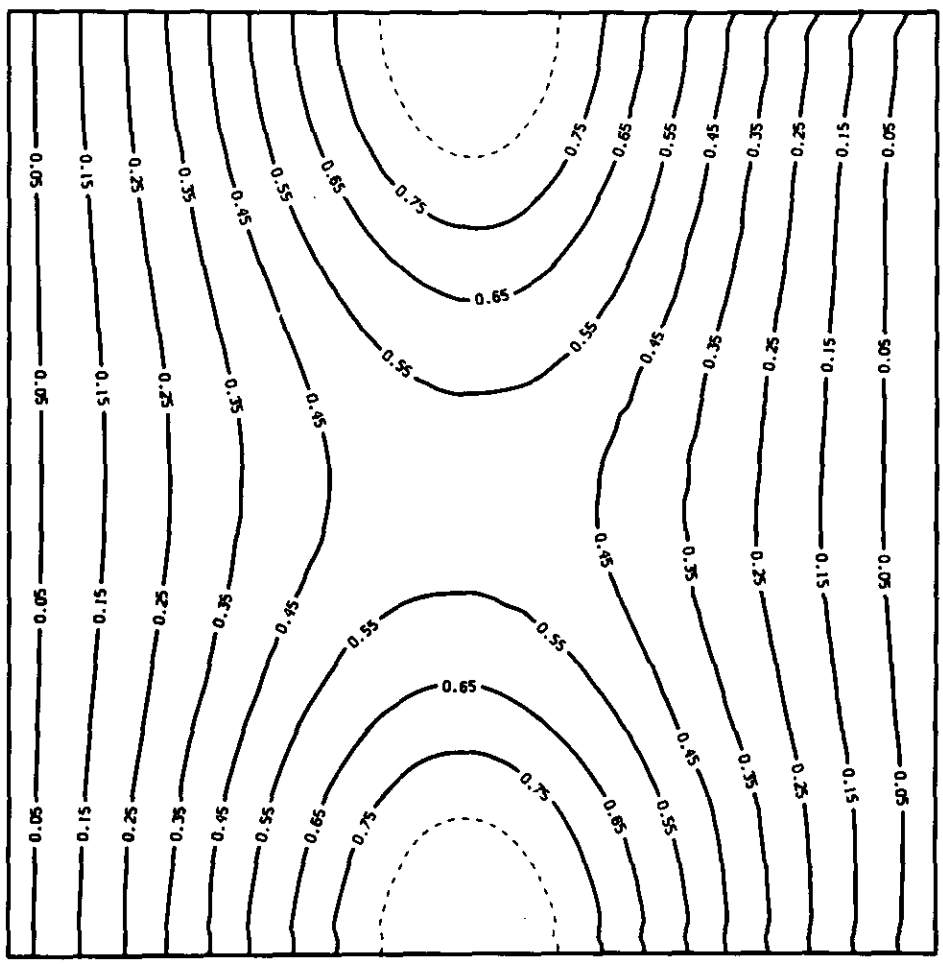

FIG. 1. Streamlines depict an eddy at $t = 2.2L/u_0$ that is formed in the flow by a Kelvin–Helmholtz instability. The domain is periodic in y (vertical) and bounded by rigid walls in x, and resolved by an adaptive grid with 120×120 zones.

created by a change in the topology of the magnetic field called magnetic reconnection, which is caused by resistive diffusion. Reconnection occurs at an accelerated rate in the region of intense current, Fig. 3. The current is amplified as the magnetic field is twisted and stretched by the fluid motion. In fact, it is conjectured that the rate of reconnection is independent of the resistive diffusion.

Overlay plots of the magnetic field and the grid calculated on a 60×30 grid are shown in Figs. 4–6 at $t = 1.67L/u_0$ for three cases; (a) Fig. 4 with directional control only ($w = 1$, $\Gamma = 0.95$); (b) Fig. 5 with an adaptive grid ($w = n\mathbf{J}$, $\Gamma = 0$); (c) and Fig. 6c with an adaptive grid and directional control ($w = n\mathbf{J}$, $\Gamma = 0.95$). n is the number of computation particles per cell. For alignment with the magnetic field, the reference vectors in Eqs. (3.5a), (3.5b) are $\mathbf{A} = \mathbf{b}'$, and $\mathbf{B} = \mathbf{b}' \times \hat{\mathbf{z}}$, where $\mathbf{b}'$ is the scaled magnetic field, $\mathbf{b}' = \mathbf{b}/|\mathbf{b}|_{\max}$. We note that the magnetic field is zero at the neutral current sheet. In the adaptive cases, the weight function is smoothed so that the minimum length scale of variation is 2δ. Natural boundary conditions, are applied by adjusting the positions of nodes on the boundary so that Eq. (1.14) is satisfied.

In case (a) with directional control only, Fig. 4, the inhomogeneous terms in Eqs. (3.5a), (3.5b) cause grid points to cluster in regions of large curvature or divergence of the scaled field, not only across the magnetic field, but along it as well. This causes a clustering of grid points in the center of the mesh. The alignment of the vertical grid lines with the magnetic field is evident, as is the tendency for horizontal grid lines to be perpendicular to the magnetic field lines. In case (b) with an adaptive mesh, Fig. 5, the grid clusters to resolve the current regardless of the direction of the magnetic field, and the zones are noticeably more skewed compared with case (a). Zoning in the mixing layer is uniformly fine, with little clustering in the y-direction. In case (c) with adaptivity and directional control, Fig. 6, the grid tends to align with the magnetic field direction.

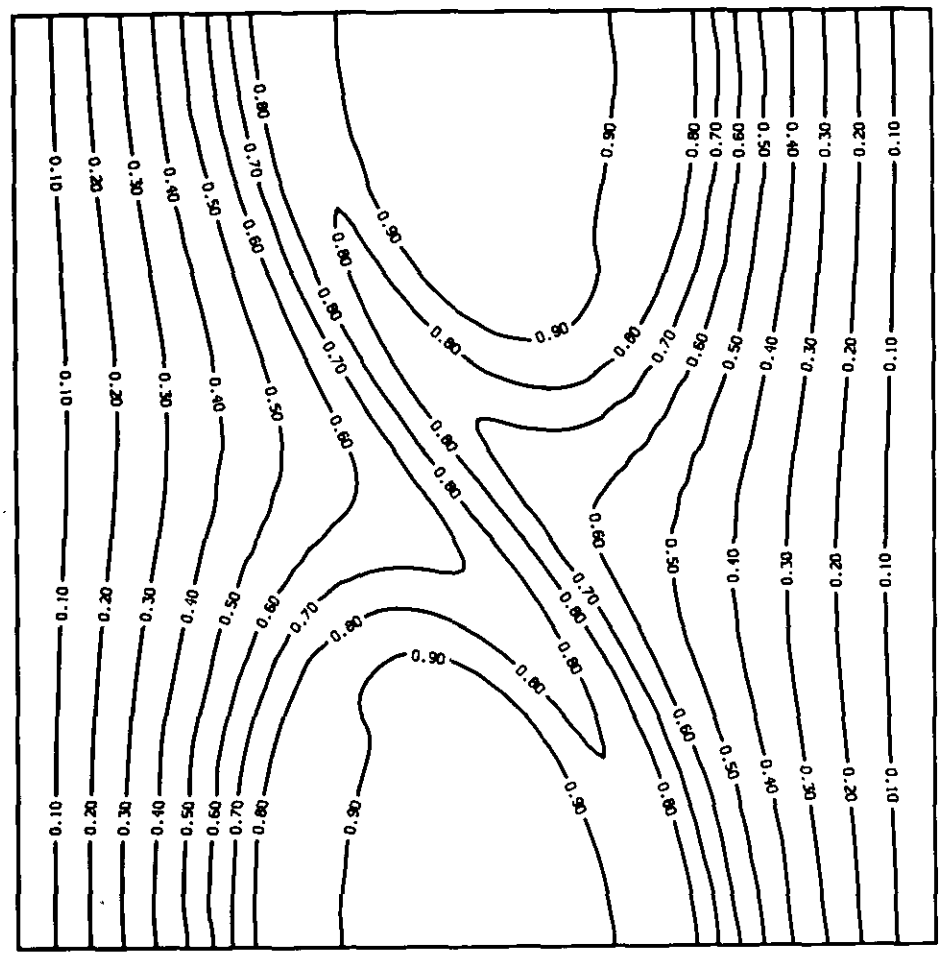

FIG. 2. Magnetic field lines enclose the eddy in Fig. 1. The closed field lines have been formed by magnetic reconnection.

Figure 6a corresponds to $t=0$, 6b to $t=0.83L/u_0$, 6c to $t=1.67L/u_0$, and 6d to $t=2.5L/u_0$. The alignment of the grid and the magnetic field is very good through Fig. 6c, but in 6d, after reconnection has formed closed field regions like those shown in Fig. 2, alignment in the center is no longer possible. Nevertheless, there is no evidence of deterioration in the quality of the calculation, nor is there any tendency for the grid generator to fail. Compared with Fig. 5, the clustering in 6c results in finer zoning near the center of the domain, but coarser zoning near the top and bottom.

The value of directional control in this problem may be assessed by comparing the calculated dissipation of the magnetic field,

$$h=\int_D d^3x\,\eta\mathbf{j}^2, \qquad \mathbf{j}=\nabla\times\mathbf{b}, \tag{4.4}$$

for a sequence of adaptive grids (b), of adaptive grids with directional control (c), and of uniform Eulerian grids (d) with increasing resolution. The value of h increases with increasing resolution until the calculation converges and correlates well with other measures of convergence. To calculate h correctly, the grid must resolve gradients perpendicular to the magnetic field.

In Fig. 7, we plot the value of h against the effort required, where the effort measures the computational cost and is the product of the number of grid points and the number of time steps to reach a time $t=2.5L/u_0$. (The curves are a least squares fit of an exponential to the data, and are meant more to guide the eye than to indicate scaling.) While the effort does not include an adjustment for the cost of the grid generator, the adjustment is less than 20%. Each case is computed on at least three grids, with one grid in each sequence fine enough to yield the converged value of h (0.085 in arbitrary units). The adaptive grid (triangles) gives the same accuracy with somewhat less effort than an

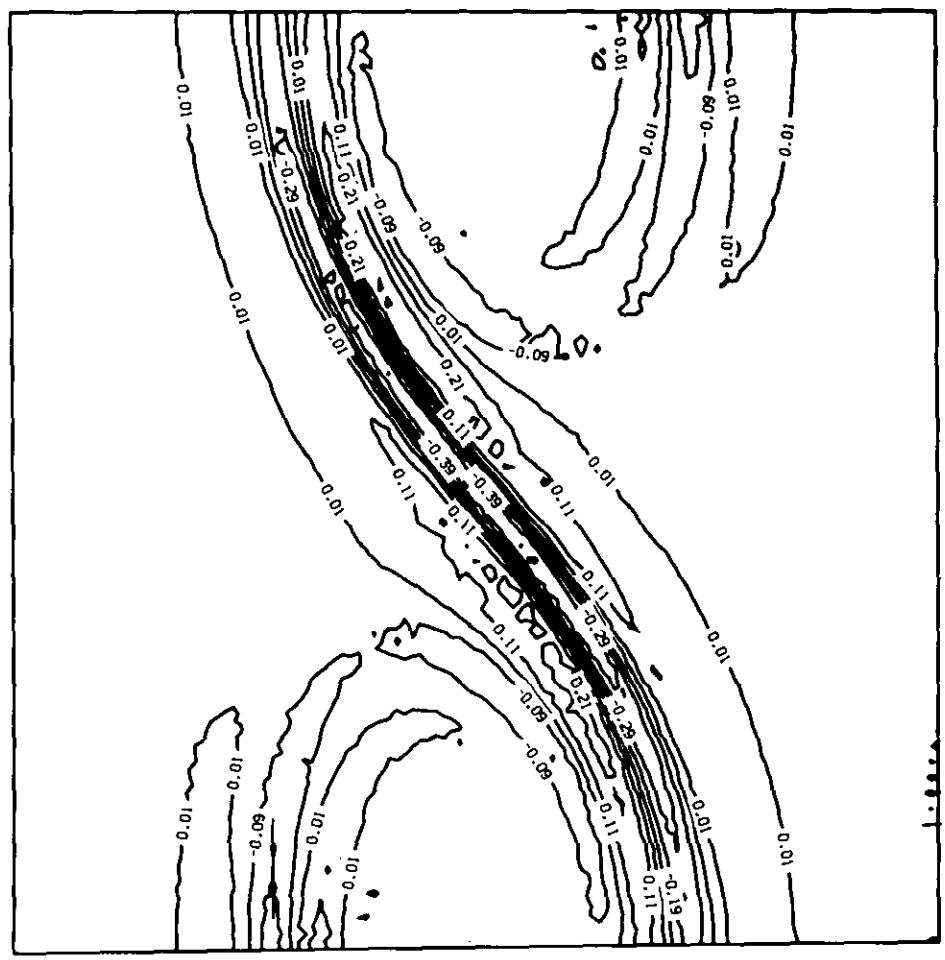

FIG. 3. Current sheets are formed by the twisting and stretching of the magnetic field in Fig. 2. The current is especially intense in the center, and there the magnetic diffusion and reconnection are occurring at an accelerated rate.

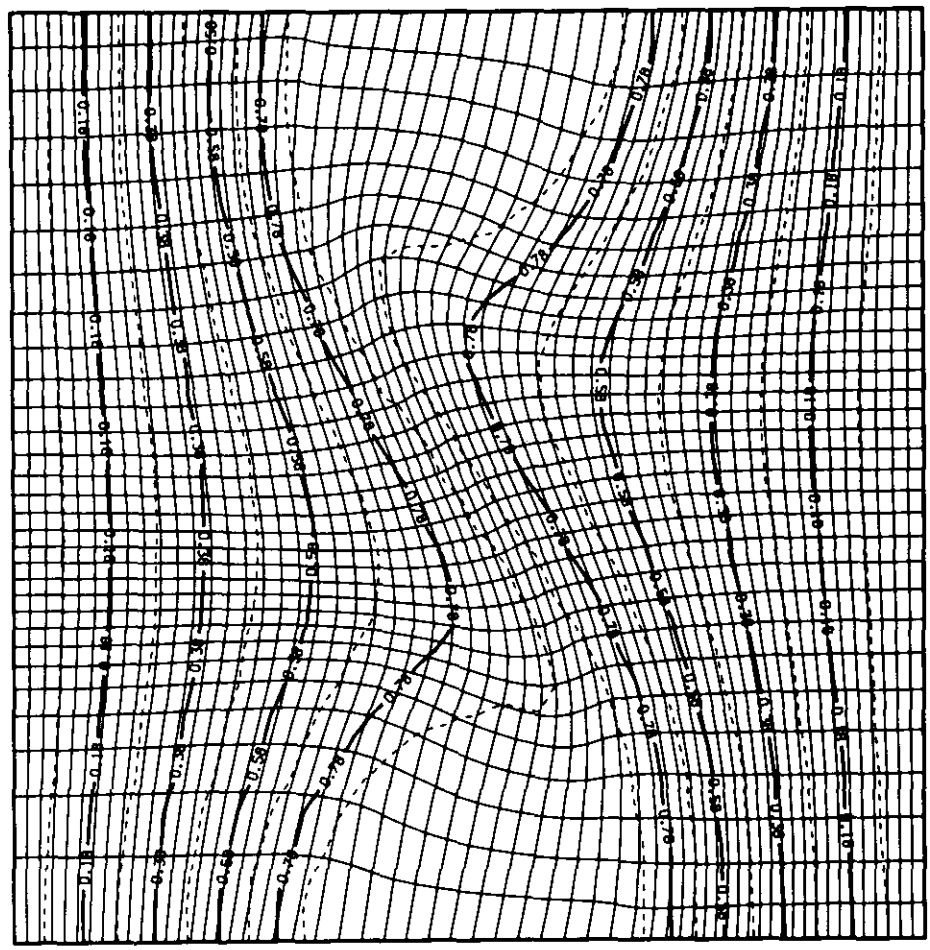

FIG. 4. Plots of magnetic field lines and of a directionally controlled computation mesh are superimposed at $t \approx 1.67L/u_0$.

Eulerian grid (squares). Convergence is nearly reached with a 60×60 adaptive grid. A converged calculation on an Eulerian grid with 120×120 zones at three times the cost is shown, but estimates of the dissipation scale length indicate a 90×90 grid would suffice. The smaller zones in the adaptive grid decrease the time step compared with the Eulerian grid, so that an adaptive grid with the same number of zones requires more effort than an Eulerian grid. Thus, the decrease in computational effort gained by using an adaptive grid appears to be only 25%.

Dramatic decreases in cost over Eulerian calculations are achieved using adaptive grids with directional control (circles). A converged result requires about 10% of the effort required with an Eulerian grid. The dramatic decrease results in part from halving the number of grid points in the y direction in (c) over (b), which not only halves the number of grid points but also increases the time step. (The time step is roughly equal to the fluid transit time across a cell. Since the dominant flow is in the y direction, the time step is larger with larger grid spacing.) However, halving the number of zones in y without adaptivity or directional control gives only a slight decrease in effort, Fig. 8, for the same accuracy. Further, a comparison of the heating calculated using a 60×30 mesh indicates that directional control or adaptivity alone gives less increase in accuracy than directional control

TABLE I

The Computational Cost and Accuracy of Calculations on a 60×30 Grid with Several Grid Strategies

Mesh strategy	Heating[a]	Computational cost[b]
Eulerian	65	100
Directional	70	100
Adaptive	82	176
Directional + adaptive	100	138

[a] Percentage of converged value.

[b] Percentage of number of time steps required for Eulerian calculation.

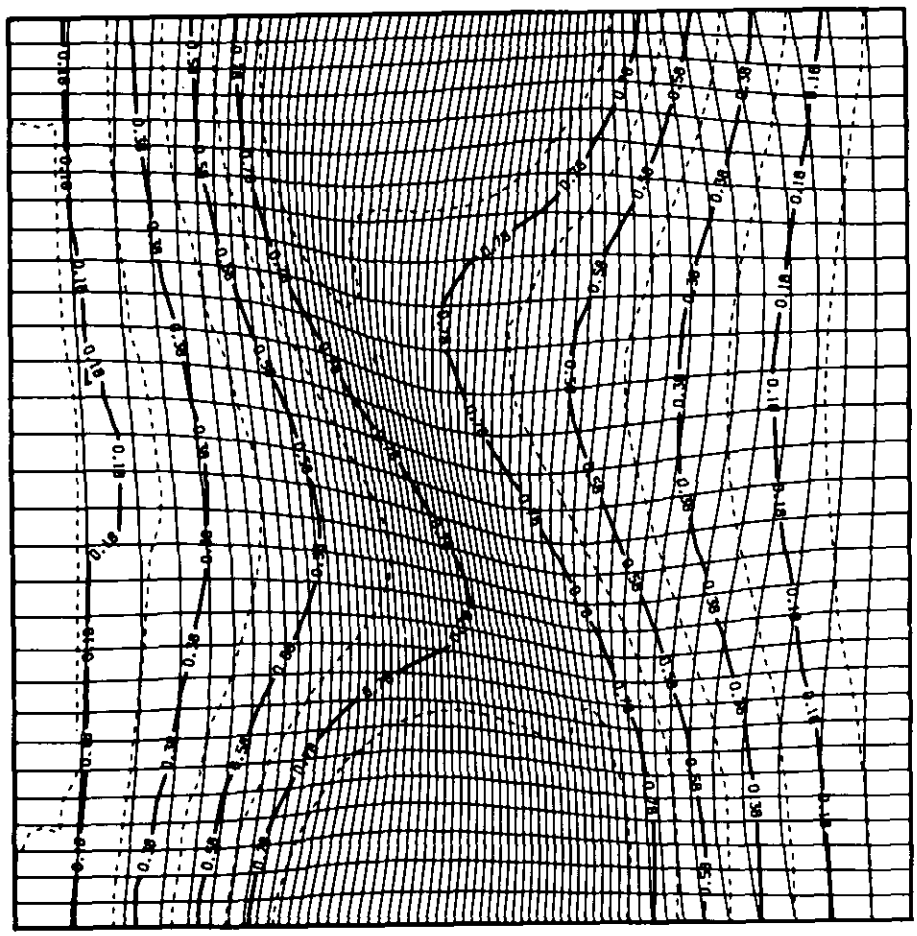

FIG. 5. Plots of magnetic field lines and of an adaptive computation mesh are superimposed at $t = 1.67L/u_0$.

and adaptivity together, Table I. Thus, we conclude that combining adaptivity and directional control is the most effective strategy for increasing computational efficiency, one that can result in dramatic savings in computer resources.

5. CONCLUSION

We have discussed harmonic function theory and explored its application to Winslow's "variable diffusion" mesh generator and a directional control functional. We have illustrated the properties of the resulting mesh generator equations when used to model unstable magnetohydrodynamic flow in two dimensions. We observe dramatic increases in computational efficiency when an adaptive grid generator with directional control is used.

Space prevents our addressing several important questions. The most obvious omission is the absence of any description of the numerical approximation of the generator equations, or of their solution. While it is certainly inconvenient to search for clues as to how this might be done in the literature, it is our observation that the methods are completely standard. One might profitably read Dvinsky, who discusses some of the less obvious issues that arise in time-dependent adaptive gridding [18], and, of course, the text by Thompson *et al.*, which discusses some of the fundamental issues in grid generation [11]. Of the greatest value in addressing implementation issues are reports with listings and examples. Unfortunately, such reports are scarce and hard to find.

Finally, we apologize for contributing here to the proliferation of papers on grid generation. There appear to be as many different approaches to grid generation as there are practitioners in the field. Review articles, such as Hawken *et al.* [9], provide useful surveys. For the potential user, however, the multiplicity of methods is still intimidating. How is he to decide which method is best for his purpose? Our best answer to this question is that the marginal utility of using an adaptive grid over using a

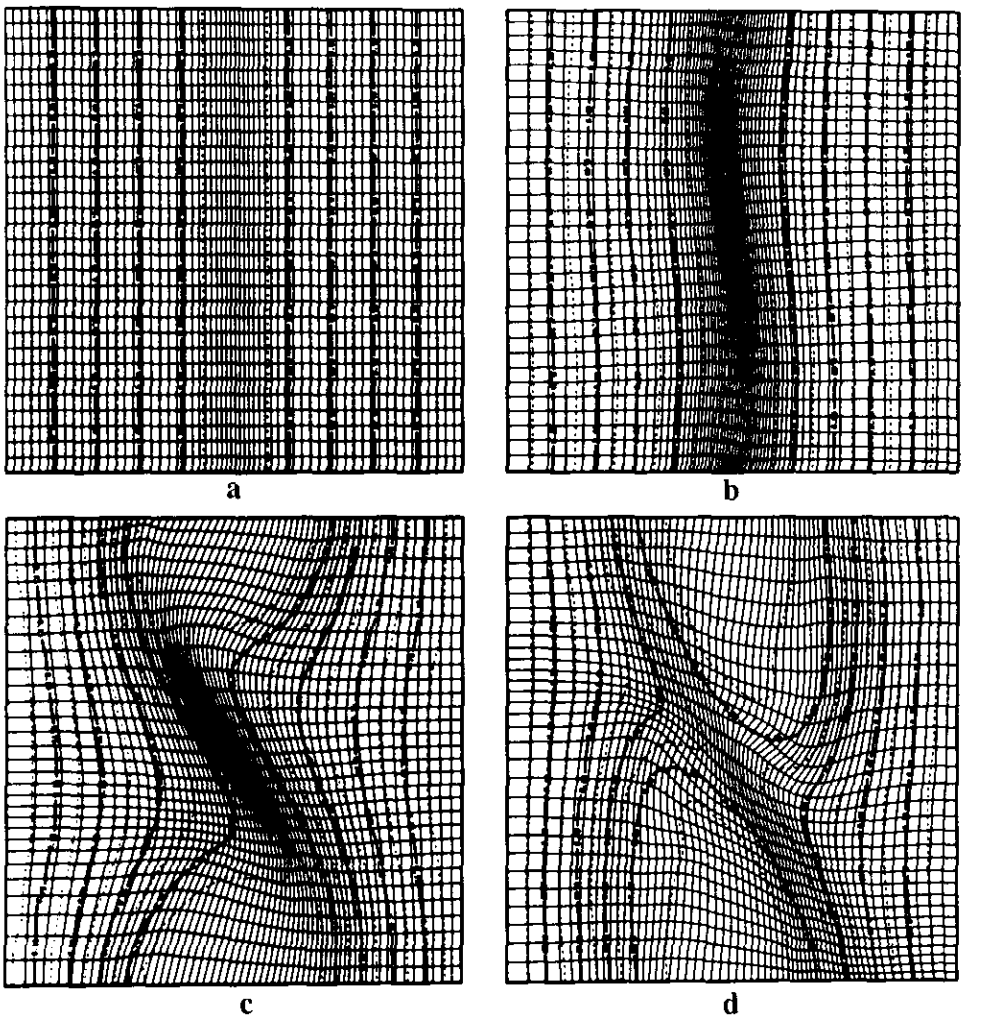

FIG. 6. Plots of magnetic field lines and of an adaptive mesh with directional control are superimposed at $t=0$, $t=0.83L/u_0$, $t=1.67L/u_0$, and $t=2.5L/u_0$ in panels a–d, respectively.

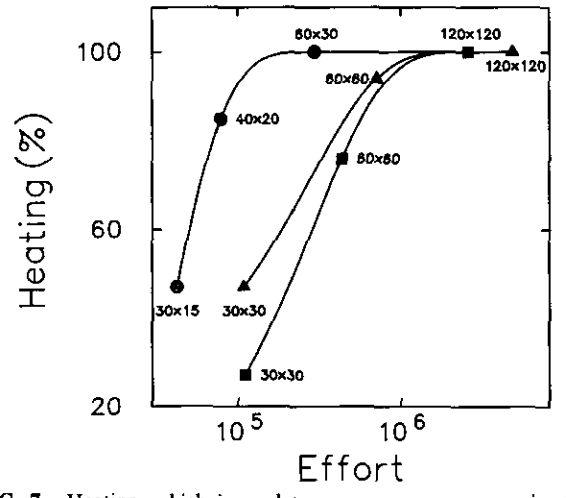

FIG. 7. Heating, which is used to measure convergence, is plotted against the effort, which increases with an increased number of grid points. An adaptive grid, (■), reduces the effort about 25% compared with an Eulerian grid, (▲), but an adaptive grid with directional control, (●), reduces the effort by 800%.

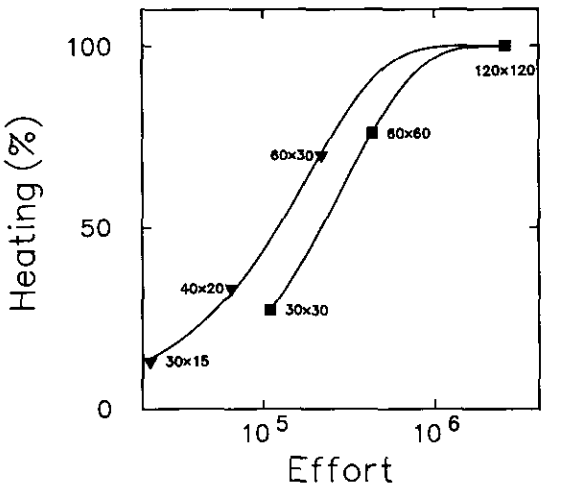

FIG. 8. Comparison of the heating calculated on two Eulerian grids shows that halving the number of zones in x is not an effective way to increase computational efficiency.

uniform grid is much greater than the marginal utility of using one method for adaptive gridding over another. It is almost always better to use an adaptive grid of any kind than to use none.

ACKNOWLEDGMENTS

We gratefully acknowledge discussions with many of our colleagues, including J. Baumgardner, J. Dukowicz, D. S. Sulsky, H. X. Vu, T. Wilson, and C. Zemach, and the support of the NASA Space Plasma Theory Program.

REFERENCES

1. R. J. Gelinas and S. K. Doss, *J. Comput. Phys.* **40**, 202 (1981).
2. I. Altas and J. W. Stephenson, *J. Comput. Phys.* **94**, 201 (1991).
3. G. Cheshire and W. D. Henshaw, *J. Comput. Phys.* **90**, 1 (1991).
4. S. McKay and J. W. Thomas, *Lectures in Applied Mathematics*, Vol. 26, (Am. Math. Soc., Providence, RI, 1990), p. 413.
5. P. K. Moore and J. E. Flaherty, *J. Comput. Phys.* **98**, 54 (1992).
6. J. U. Brackbill and J. S. Saltzman, *J. Comput. Phys.* **46**, 342 (1982).
7. H. A. Dwyer, R. J. Kee, and B. R. Sanders, *AIAA J.* **18**, 1205 (1980).
8. K. Nakahashi and G. S. Deiwert, *AIAA J.* **24**, 948 (1985).
9. D. F. Hawken, J. J. Gottlieb, and J. S. Hansen, *J. Comput. Phys.* **95**, 254 (1991).
10. C. W. Mastin and J. F. Thompson, *Numer. Math.* **29**, 397 (1978).
11. J. F. Thompson, Z. U. A. Warsi, and C. W. Mastin, *Numerical Grid Generation: Foundations and Applications* (Elsevier, New York, 1985).
12. G. Ryskin and L. G. Leal, *J. Comput. Phys.* **50**, 71 (1983).
13. D. Lee and Y. M. Tsuie, *J. Comput. Phys.* **98**, 90 (1992).
14. G. D. Kerlich and G. H. Klopfer, "Assessing the quality of curvilinear coordinate meshes by decomposing the Jacobian matrix," in *Numerical Grid Generation*, edited by J. F. Thompson (Elsevier, New York, 1982).
15. R. Liska and M. Y. Shashkov, International Symposium on Symbolic and Algebraic Computation, Bonn, Germany, 1991.
16. D. Sulsky and J. U. Brackbill, *J. Comput. Phys.* **96**, 339 (1991).
17. K. N. Christodoulou and L. E. Scriven, *J. Comput. Phys.* **99**, 39 (1992).
18. A. S. Dvinsky, *J. Comput. Phys.* **95**, 450 (1991).
19. A. M. Winslow, UCID-19062, Lawrence Livermore National Laboratory, 1981 (unpublished).
20. A. E. Giannakopoulos and A. J. Engel, *J. Comput. Phys.* **74**, 422 (1988).
21. F. B. Fuller, *Proc. Nat. Acad. Sci.* **40**, 987 (1951).
22. R. Aris, *Vectors, Tensors, and the Basic Equations of Fluid Dynamics* (Prentice–Hall, Englewood Cliffs, NJ, 1962).
23. A. A. Amsden and C. W. Hirt, *J. Comput. Phys.* **11**, 348 (1973).
24. D. A. Anderson, *Appl. Math. Comput.* **24**, 211 (1987).
25. P. R. Eiseman, *Comput. Methods Appl. Mech. Engrg* **64**, 321 (1987).
26. Y. Tu and J. F. Thompson, *AIAA J.* **29**, 2025 (1991).
27. J. U. Brackbill, D. B. Kothe, and H. M. Ruppel, *Comput. Phys. Commun.* **48**, 25 (1988).
28. Z. U. A. Warsi and J. F. Thompson, *Comput. Math. Appl.* **19**, 31 (1990).
29. F. L. Addessio, J. R. Baumgardner, J. K. Dukowicz, N. L. Johnson, B. A. Kashiwa, R. M. Rauenzahn, and C. Zemach, LA-10613-MS, Rev. 1, Los Alamos National Laboratory, 1992 (unpublished).
30. J. F. Thompson, F. C. Thames, and C. W. Mastin, *J. Comput. Phys.* **24**, 274 (1977).
31. J. U. Brackbill, in *14th International Conference on the Numerical Simulation of Plasmas, Annapolis, MD,1991*, edited by A. Mankofsky and I. Haber.
32. J. U. Brackbill, *J. Comput. Phys.* **96**, 163 (1991).
33. M. Lesieur, *Turbulence in Fluids* (Kluwer, Boston, 1990).
34. H. K. Moffatt, *Magnetic Field Generation in Electrically Conducting Fluids* (Cambridge University Press, Cambridge, 1978).